ELSEVIER

Chemical Engineering Journal 78 (2000) 61–67

Chemical Engineering Journal

www.elsevier.com/locate/cej

Feed temperature influence on the efficiency of a molecular evaporator

Ján Cvengroš[a,*], Juraj Lutišan[b], Miroslav Micov[a]

[a] *Faculty of Chemical Technology, Slovak Technical University, Radlinského 9, 812 37 Bratislava, Slovak Republic*

[b] *HighChem, Ltd., Jána Stanislava 35, 841 05 Bratislava, Slovak Republic*

Received 6 February 1999; received in revised form 22 October 1999; accepted 27 November 1999

Abstract

The temperature of a liquid entering the evaporating cylinder of a molecular evaporator is one of the important technological parameters that determine an evaporator's operation. In this model study, the effect of the feed temperature on the film surface temperature on the evaporating cylinder was observed for various liquid loads and for various differences between evaporation surface temperatures and feed temperatures. The length of the evaporating cylinder measured from the top, along which the temperature on the film surface reaches a steady-state, constant value (asymptotic temperature) increases with decreasing feed temperature, with rising the liquid load and with rising evaporator cylinder temperature. Along this length, which may reach up to several hundred millimetres, evaporation occurs at a reduced rate which corresponds to the real temperature on the film surface. Therefore, it is useful to gently preheat the feed before it enters the evaporator in appropriate front-end heat exchangers to a temperature close to the asymptotic temperature.

Keywords: Molecular evaporator; Feed temperature; Molecular distillation; Evaporator efficiency

1. Introduction

Molecular or short-path distillation is characterized by a short exposure of the distilled liquid to elevated temperatures, high vacuum in the distillation space and a small distance between the evaporator and the condenser. The short residence time of the liquid on the evaporating cylinder, on the order of a few seconds to tens of seconds, is guaranteed by distributing the liquid in the form of a thin film of even consistency. By considerably reducing the pressure of non-condensable gas in the evaporator to the 10^{1}–10^{-1} Pa level, a reduction of the distillation temperatures by as much as 250°C can be obtained. The combination of a small distance between evaporator and condenser (20–70 mm) with a high vacuum in the distillation gap results in a specific mass transfer mechanism with evaporation outputs as high as 20–40 g m^{-2} s^{-1}. Under these conditions, e.g., short residence time and low temperature, distillation of heat-sensitive materials is accompanied by only negligible thermal decomposition and proceeds at rates which can be technologically utilized.

The scheme of an apparatus for falling film molecular distillation is shown in Fig. 1. It consists of a cylindrical evaporator surrounded by a closely positioned condenser jacket. The distilled liquid flows down the evaporating cylinder in the form of a film, it is partly vaporized and evaporated molecules condense on the condenser. If both films are much thinner than the evaporator and condenser radii, they can be regarded as planar.

The temperature of the liquid entering the peripheral of the evaporation cylinder of a molecular evaporator represents an important operational parameter. Practical experience over many years with the operation of molecular evaporators have shown that the optimum temperature of the entering de-gassed liquid should not differ too much from the working temperature inside the evaporator. This results in evaporation at a non-reduced rate from the very first moment the distilled liquid gets onto the evaporation surface, without using the evaporation surface to post-heat liquid to the operation temperature. On the other hand, molecular distillation is used to process thermally sensitive substances which do not tolerate long-term exposures to increased temperature in the presence of oxygen, and which are not easy to heat to the desired temperature on front-end heat exchangers without the risk of suffering thermal damage. The heating of liquid in film form is relatively efficient and, above all, careful; evaporator with liquid film as heat

* Corresponding author. Tel.: +421-7-59325-531; fax: 421-7-52493-198.
E-mail addresses: cvengros@chtf.stuba.sk (J. Cvengroš), lutisan@highchem.com (J. Lutišan), cvengros@chtf.stuba.sk (M. Micov)

1385-8947/00/$ – see front matter
PII: S1385-8947(99)00159-X

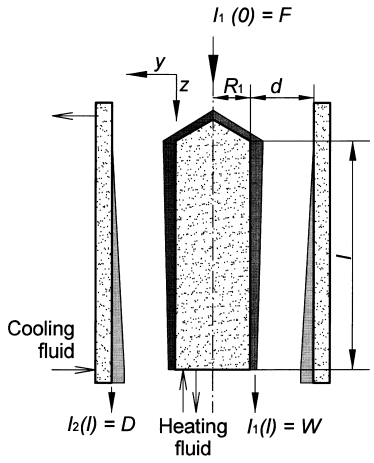

Fig. 1. Scheme of falling film molecular evaporator.

exchanger, however, is at least problematic as far as capital investment costs are concerned.

The aim of the present paper is to investigate, in model studies, the development of temperatures on the film surface along the length of the evaporator under steady-state conditions depending on the peripheral liquid load of evaporating cylinder, on the temperature differences between evaporation surface temperature and entrance liquid temperature (feed temperature), as well as on the temperature of evaporation surface. The study is expected to provide information on the portion of evaporation surface lost for liquid heating upon feeds with temperatures lower than that of the evaporator. Experimental data on film surface temperatures are not available since the film is only several tenths of a millimeter thick.

Several studies report the results of molecular distillation modeling. Bose and Palmer [1] have given reasons for a separation efficiency decrease by distillation in a jet tenzimeter. This decrease is caused by both concentration and temperature gradients in the distilled liquid mixture as a consequence of intense evaporation. Kawala and Stephan [2] have simulated the processes in falling film with an adiabatic regime. Bhandarkar and Ferron [3] have presented a description of heat and mass transfer in liquid film on the conical evaporator of a centrifugal still. Batistella and Maciel [4] have compared in model study the performance and efficiency of the falling-film and centrifugal distillators, respectively. Toei et al. [5] have studied the influence of inert gas pressure on the process of molecular distillation.

2. Theoretical

The assumption that distilled liquid consists of one component will be used in our work. In this case, the parameters for heat transfer under steady-state conditions are described by three fundamental balance equations: the Boltzmann equation for mass transfer in the vapor phase, the Navier–Stokes equation for film flow in the gravity film and the thermal balance equation.

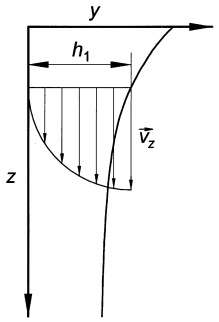

Fig. 2. Scheme of the film shape on the evaporator.

A scheme of the film flow on the evaporating cylinder with the co-ordinate system orientation specified is shown in Fig. 2.

A physical model of a set of balance equations for molecular distillation in a short-path evaporator was suggested in our previous papers [6,7]. A laminar liquid film on evaporator and condenser is assumed, with the inter-molecular collisions in the vapor phase being neglected. The set of balance equations published in [6] also holds for this case, including the temperature dependence of liquid viscosity, differences in evaporator wall temperature T_w, and differences in feed temperature T_F. The existence of a steady-state solution is assumed.

The system of the balance equations then is as follows:

1. Navier–Stokes equation for velocity field

$$(\vec{v}\text{grad})\vec{v} = \nu\nabla^2\vec{v} + \vec{g} \tag{1}$$

in our case, $\vec{v} = (0, 0, v_z(y, z))$, $\vec{g} = (0, 0, g)$

$$v(z)\partial_y^2 v_z(y, z) = -g$$

thus yielding Nusselt's solution to velocity field:

$$v_z(y, z) = \frac{gh_1(z)^2}{\nu}\left(\frac{y}{h_1(z)} - \frac{y^2}{h_1(z)^2}\right) \tag{2}$$

2. Balance equation for heat transfer:

$$v_z\partial_z T(y, z) = \vartheta(\partial_y^2 + \partial_z^2)T \tag{3}$$

where

$$\vartheta = \frac{\lambda}{c_p\rho} \tag{4}$$

The heat transfer by convection along the z-axis (term $\vartheta\partial_z^2 T$) will be neglected in comparison with the other two terms because of the liquid flow along the z-axis. Then, the Eq. (3) can be written as:

$$v_z\partial_z T(y, z) = \vartheta\partial_y^2 T \tag{5}$$

Initial and boundary conditions are

$$T(y, 0) = T_F \tag{6}$$

$$T(0, z) = T_w \tag{7}$$

$$\lambda \partial_y T|_{y=h} = -\Delta_{\text{evp}} H k \tag{8}$$

where

$$k = \frac{p^0(T_s(z))}{\sqrt{2\pi R_1 M T_s(z)}} \tag{9}$$

is the surface evaporation rate for ideal liquid.

The dependence of flow I on coordinate z is given by continuity equation

$$\partial_z I(z) = -2\pi R_1 k \tag{10}$$

The initial condition is:

$$I(0) = F = \frac{2\pi R_1 \Gamma \rho}{3.6 \times 10^5 M} \tag{11}$$

The set of Eqs. (5) and (10) with the boundary condition specified by Eqs. (7) and (8) was solved numerically. The calculation was performed with a step of Δz. The state for z=0 is determined by the initial conditions (6) and (11). In each step, the value of flow was determined from the value of I in previous step using Taylor's approximation [8] of Eq. (10):

$$I(z + \Delta z) = I(z) - 2\pi R_1 k \Delta z \tag{12}$$

The film thickness was computed from the known value of $I(z+\Delta z)$

$$h_1(z + \Delta z) = \sqrt[3]{\frac{3\nu}{2\pi R_1 g c} I(z + \Delta z)} \tag{13}$$

The partial differential equation (5) with boundary conditions (7) and (8) was solved using the networks method. In our case, the implicit, always stable Crank–Nicholson scheme [9] was used for the transformation of Eq. (5) into a discrete form. The discretization scheme is shown in Fig. 3, the value of temperature in the node i, j was calculated from the set of linear equations:

$$\frac{T_i^j - T_{i-1}^j}{\Delta z} = \frac{1}{2}\frac{\vartheta}{v_z}\left(\frac{T_i^{j+1} - 2T_i^j + T_i^{j-1}}{\Delta y^2} + \frac{T_{i-1}^{j+1} - 2T_{i-1}^j + T_{i-1}^{j-1}}{\Delta y^2}\right) \tag{14}$$

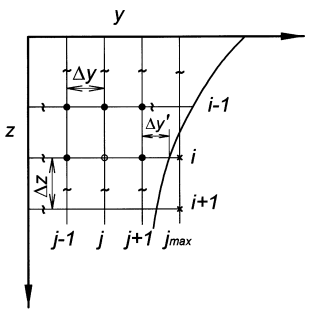

Fig. 3. Scheme of the Crank–Nicholson net method.

The initial conditions are given by the known temperature profile in the first layer (for i=0) according to Eq. (6). The boundary conditions on the evaporator's wall are specified by Eq. (7). This differential boundary condition (8) was replaced by a difference. Therefore, the relation between the nodes $i, j_{\max-1}$, and $i, j_{\max}$ (in Fig. 3, the node $i, j_{\max-1}$ is identical to the node $i, j+1$) can be expressed by the equation:

$$\frac{T_i^{j_{\max}} - T_i^{j_{\max-1}}}{\Delta y} = -\frac{\Delta_{\text{evp}} H k}{\lambda} \tag{15}$$

The value of evaporating rate k depends on the surface temperature T_s the value of which has not been determined yet. For simplicity, the value of the surface temperature from the previous step of the solution was taken.

The actual film surface temperature T_s (a fictive surface temperature in the node $i, j_{\max}$ situated outside the film is obtained by solving the above set of equations) is obtained again through the linear substitution of the boundary condition (8):

$$T_s = T_i^{j_{\max-1}} - (h_1 - \Delta y j_{\max-1})\frac{\Delta_{\text{evp}} H k}{\lambda} \tag{16}$$

For comparison, our model, as described in previous studies [6,7], was applied under the same conditions. Eqs. (1)–(11) make up the basis of this approximative model, the modeled set, however, is composed of a two-component mixture, and there is a concentration gradient in the film. The model also includes the re-evaporation of molecules returning from the condenser to the evaporating cylinder; the condenser is described in the same way as the evaporating cylinder. In these studies, it was assumed that the dependence of temperature on the y-coordinate is linear, and the dependence of the concentration of one of the components on the y-coordinate is parabolic. This marks the difference between this approximative model and the non-approximative model described above. In this case, we succeeded in re-arranging the set of partial differential equations to obtain a set of ordinary differential equations and several non-linear equations which were solved numerically using the Runge–Kutta method. For a one-component mixture, the solution described in [6,7] is simplified into Eq. (10) with the initial conditions (6) and (11) and the equation determining the surface film temperature:

$$T_s(z) = T_w + h_1(z)\frac{\Delta_{\text{evp}} H k(T_s(z))}{\lambda} \tag{17}$$

The only complication is the determination of the evaporation rate k, which depends on the surface temperature T_s ought. The surface temperature is therefore determined by iteration.

All calculations were performed by a PC computer (Pentium Pro 180 MHz, 64 MB RAM with the Windows NT 4.0 Workstation operating system). Calculation programs employed were developed and debugged using the Visual C++ 5.0 programming language.

Table 1
Physical parameters of di-*n*-butylphthalate (DBP)

M (g mol^{-1})	$\log p^0$ (Pa)	$_{evp}H$ (kJ mol^{-1})	c_p (J mol^{-1} K^{-1})	ρ (kg m^{-3})	$\log \eta$ (Pa s)
278.35	12.7−(4450/T)	85.6	583	1294.6−0.839T	(1487.6/T)−6.79

3. Results and discussion

As already mentioned, film surface temperature T_s represents the determining factor for the evaporation process. The aim of the study was to determine the development of film surface temperature along the height of the evaporator in dependence on peripheral liquid load and on the liquid entrance temperature. Di-*n*-butylphthalate (DBP) was used as model substance; its physical parameters are in Table 1. The evaporation cylinder was 30 mm in diameter, the temperature at its surface was 90°C (T_w=363 K) or 110°C (T_w=383 K), distance evaporator–condenser was 30 mm. The evaporator length was not limited.

Fig. 4 shows the dependence of film thickness on co-ordinate z identical to the evaporation cylinder axis starting at its top according to Fig. 1. For various feed temperatures T_F, film thickness at z=0 is given by relationship (13) in Nusselt's approximation. Film thickness strongly decreases with the increasing feed temperature, due to both the temperature dependence of viscosity and evaporation. Different relaxation lengths for film thickness have been stated for various feed temperatures. Relaxation length means the distance from the evaporator top at which the given parameter (film thickness, temperature) reaches asymptotic value. So, for T_F=353 K, relaxation length is about 50 mm from evaporator top, for T_F=313 K, this variable equals about 100 mm.

The isothermal map in Fig. 5 shows a strong drop in film thickness with the increasing value of co-ordinate z and growth of temperature in the same sense. Both parameters, film surface temperature and film thickness, have approximately identical relaxation lengths in the conditions used,

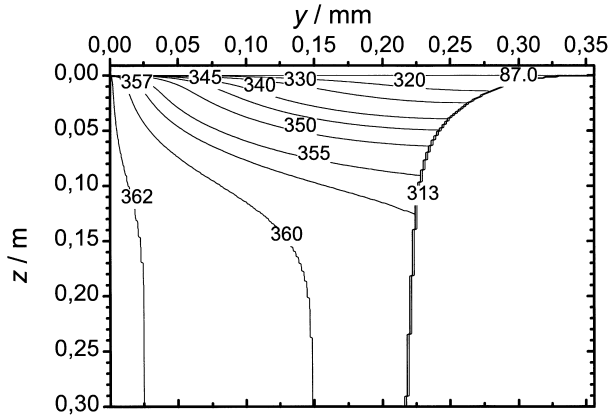

Fig. 5. Temperature map of film interior. Γ=6 l h^{-1} dm^{-1}, T_F=313 K, T_w=363 K.

i.e., both isotherms turn parallel as soon as a steady-state film thickness has formed. At distances larger than relaxation length, the temperature field in the direction perpendicular to the cylinder axis has a linear course. This also confirmed the assumption presented in our previous paper [6] on the negligible effect of convective flow on heat transfer in thin laminar films.

Fig. 6 shows the development of film surface temperature T_s as a function of z for different feed temperatures T_F for Γ=6 l h^{-1} dm^{-1}. It is evident from the figure, that all the different feed temperatures have the same asymptotic temperature of film surface, T_s=358 K for the example given, with T_w=363 K. Various entrance feed temperatures apparently have various relaxation lengths. For the given example, the temperature difference T_s and T_w is about 5 K, which

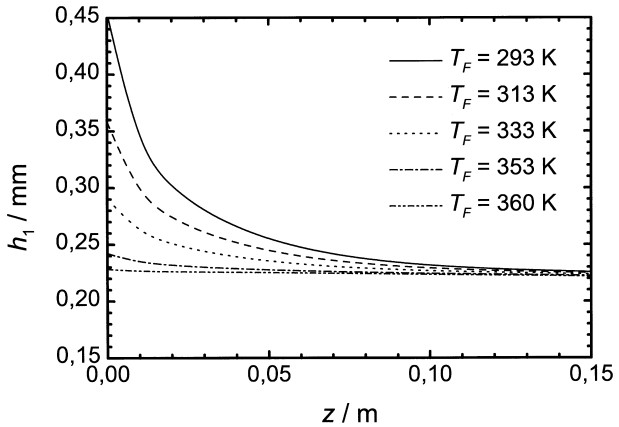

Fig. 4. Position dependence of film thickness for different feed temperatures. F=6 l h^{-1} dm^{-1}, T_w=363 K.

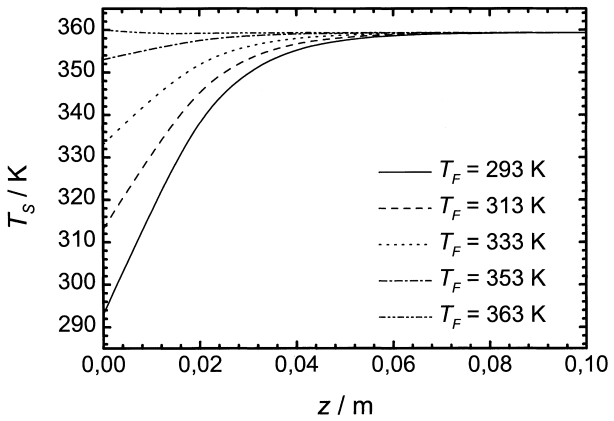

Fig. 6. Position development of film surface temperature for various feed temperatures, Γ=6 l h^{-1} dm^{-1}, T_w=363 K.

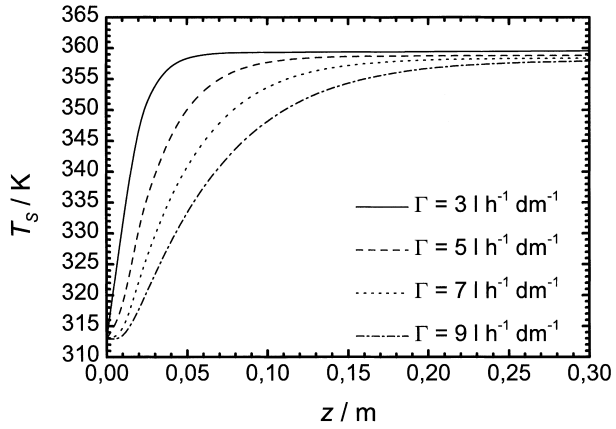

Fig. 7. Position development of film surface temperature for various liquid loads, T_F=313 K, T_w=363 K, F=31 h^{-1} dm^{-1}.

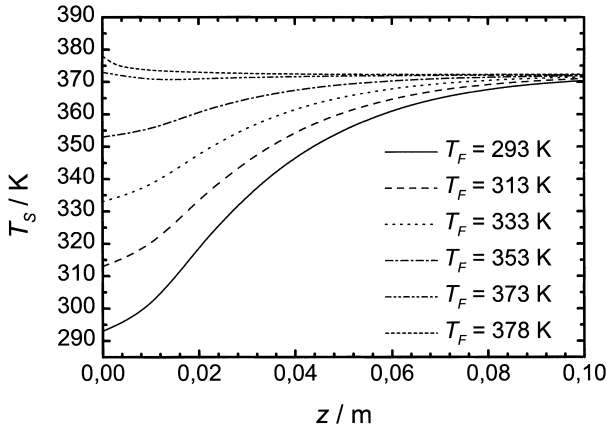

Fig. 9. Position development of film surface temperature for various feed temperatures. Γ=61 h^{-1} dm^{-1}, T_w=383 K.

corresponds, at a film thickness of about 0.22 mm, to a gradient as high as 23 K mm^{-1}. Qualitatively, this result is in accordance with our previously published results [6,7], and is connected with the relatively low thermal conductivity of liquid and with evaporation.

Further, the film surface temperature dependence T_s was studied as a function of z for various feeds at T_F=313 K (Fig. 7). In this case, the function course is as expected. Films at smaller liquid loads have higher asymptotic temperatures and shorter relaxation lengths per film thickness unit. This is connected with smaller film thickness at smaller liquid loads. Film thickness, however, is not only dependent on the liquid load and feed temperature but it also decreases with increasing evaporation. Relaxation length per temperature is relatively large, reaching at higher liquid loads several hundred millimeters for insufficiently pre-heated feeds.

Figs. 8 and 9 were obtained using the same input parameters for the calculation as in Figs. 4 and 6 with the exception of T_w which is higher by 20°C in Figs. 8 and 9. This enabled us to mutually compare both cases.

Fig. 8 shows feed temperature dependence of film thickness along the evaporation cylinder for Γ=61 h^{-1} dm^{-1} and higher wall temperature T_w=383 K. It is evident from the figure that asymptotic temperature is higher (372 K) and asymptotic film thickness smaller (about 0.18 mm) at increased T_w. This is a consequence not only of lower viscosity but also of greater decrease in the amount of liquid at higher evaporation rates. In this case, temperature gradient in film has a value of about 60 K mm^{-1}.

Fig. 9 shows a situation analogous to that in Fig. 6, however with T_s-T_w being markedly larger for higher T_w. This is connected with the substantially higher evaporation rate from the liquid surface and its cooling down. The asymptotic temperature is higher at increased T_w (372 K at T_w=383 K and 358 K at T_w=363 K). The relaxation length for T_s increases from 50 to 100 mm at higher T_w.

Fig. 10 shows the development of the film surface temperature T_s along the evaporator height for various liquid loads at constant feed temperature (T_F=313 K). Fig. 10 is comparable with Fig. 7 which has the same input parameters, but its evaporator temperature is T_w=363 K. Besides increasing the asymptotic temperature, which is naturally different for each liquid load, a decreased relaxation length

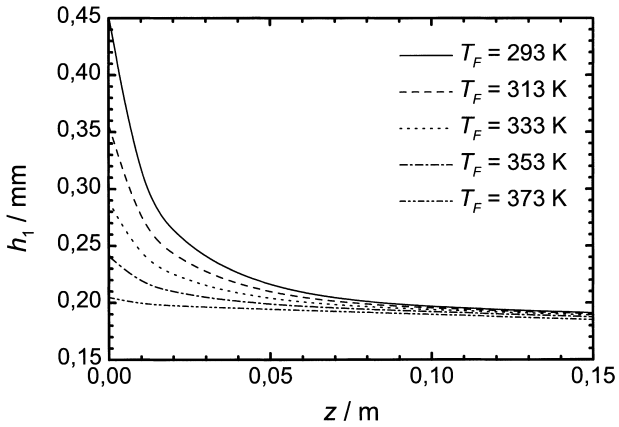

Fig. 8. Position development of film thickness for various feed temperatures. Γ=61 h^{-1} dm^{-1}, T_w=383 K.

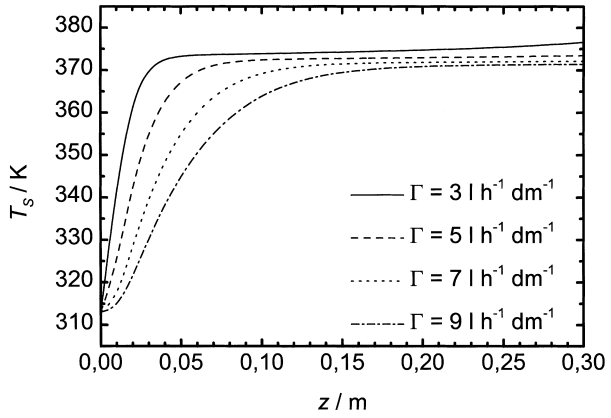

Fig. 10. Position development of film surface temperature for various liquid loads. T_F=313 K, T_w=383 K.

for the given Γ is found, resulting particularly from lower viscosity. Asymptotic temperature values are governed by physical properties of the distilled liquid.

4. Comparison of the two models

A linear development of temperature along the *y* axis was assumed in our previous paper [6]. This approximation was justified given that film thickness and liquid rate along the *z* axis are small (neglecting the convection member). This assumption markedly facilitated solution of the system of balance equations in paper [6]. Results of the model study presented herein have confirmed the justification of the above assumption. Fig. 11 shows the temperature development on film surface through complete evaporation, calculated on the original approximative model and with a non-approximative solution of temperature development along the *y* axis. If T_F is approximately equal to the asymptotic temperature, surface temperature from the approximative model is effectively identical to the non-approximative solution. If, however, T_F is markedly smaller than asymptotic temperature, both models provide different values for relaxation length.

This consideration is also confirmed by Fig. 12 which shows film thickness along the evaporator height for two feed temperatures. Also here, it is evident that at T_F=373 K, the approximative model results in a film thickness which is effectively identical to that yielded by the non-approximative model. There, film thickness is only reduced due to evaporation. At T_F=313 K, there is a marked reduction in the film thickness in the surroundings of the top of the evaporating cylinder, mainly due to the decreasing viscosity. Further decrease of $h(z)$ function is then due to evaporation.

Fig. 13 shows the dependence of the evaporated portion of feed *D/F* on coordinate *z*. In this case, the approximative model also has identical solutions to the non-approximative model for T_F=373 K. If feed temperature is markedly lower than wall temperature, the non-approximative solution shows smaller evaporation, the two relations being parallel to each other. This shift is due to a markedly smaller evaporation within the interval $z\ (0, z_{relax})$. This zone may therefore be understood as the film heating zone.

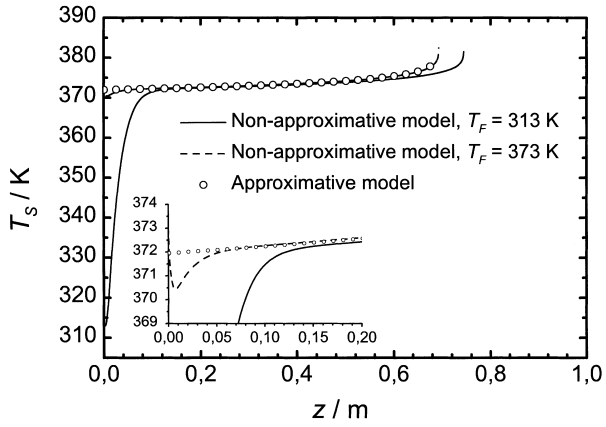

Fig. 11. Temperature development on film surface for two models. Γ=31 h^{-1} dm^{-1}, T_w=383 K.

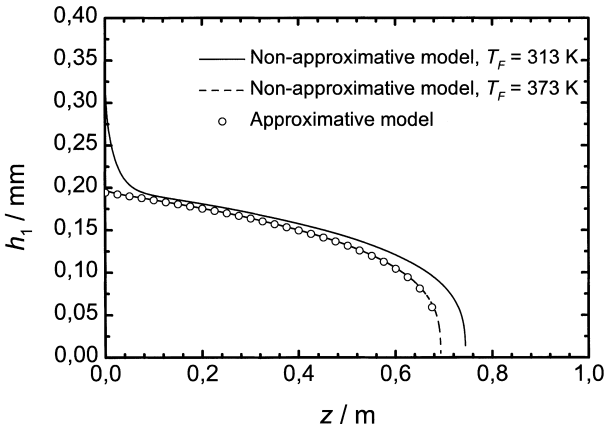

Fig. 12. Film thickness along the evaporator height for two models. Γ=31 h^{-1} dm^{-1}, T_w=383 K.

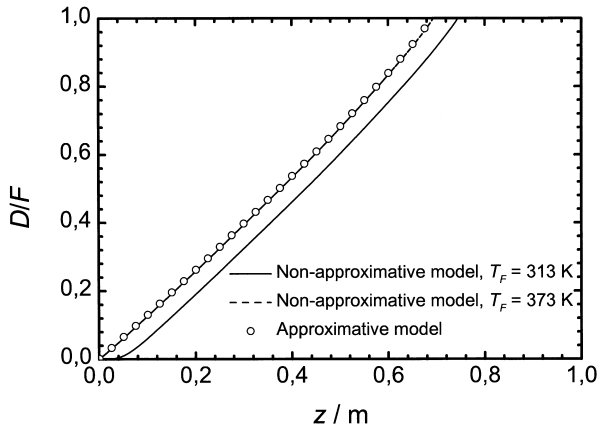

Fig. 13. Position development of evaporation degree for two models. Γ=31 h^{-1} dm^{-1}, T_w=383 K.

5. Conclusion

The results of the model study point to the advantages and efficiency of feed pre-heating to temperatures close to that of film surface under steady-state conditions (asymptotic temperature) for the given operating conditions, prior to its entering the evaporation surface. If this is not the case, a portion of evaporation surface is used to mainly post-heat liquid, and evaporation in this zone is slowed down corresponding to the real temperature of the film surface. The length of the evaporation cylinder from the evaporator top downwards where such processes are active is larger the larger the liquid load and the lower its temperature and/or the larger the difference between feed temperature and film surface temperature. At higher wall temperatures and constant liquid load as well as

at constant feed temperature, relaxation length increases. As shown by comparison of the film surface temperature development for approximative and non-approximative models, both models yield identical asymptotic temperatures. There is a substantial temperature gradient between wall temperature and film surface temperature even under steady-state conditions as soon as asymptotic temperature is achieved; the gradient represents several tens of $K\,mm^{-1}$ and is mainly determined by the physical parameters of the liquid (thermal conductivity, viscosity). Film surface temperature is a crucial factor for the evaporation rate, and it represents the operation temperature in the evaporator. There is no reason for feed pre-heating beyond that temperature.

Feed pre-heating also has additional technological importance as it enables intensive degassing of feed in expansion elements prior to getting to the evaporation surface, and reduces the risk of splashing. It should be stressed that the feed pre-heating has to be thrifty in adequate heat exchangers without large temperature differences and without the presence of oxygen (in vacuum), thus reducing the risk of thermal damage to the distilled liquid.

6. Nomenclature

c_p	thermal capacity ($J\,kg^{-1}\,K^{-1}$)
c	molar concentration ($mol\,m^{-3}$)
D	distillate ($mol\,s^{-1}$)
d	distance evaporator–condenser (m)
F	feed ($mol\,s^{-1}$)
g	gravity ($9.81\,m\,s^{-2}$)
h_1	film thickness (m)
i	discrete index in the direction of z coordinate
I	flow ($mol\,s^{-1}$)
I_1	flow on evaporator ($mol\,s^{-1}$)
I_2	flow on condenser ($mol\,s^{-1}$)
j	discrete index in the direction of y coordinate
k	rate of evaporation ($mol\,m^{-2}\,s^{-1}$)
l	evaporator length (m)
M	molar weight ($kg\,mol^{-1}$)
p^0	pressure of saturated vapour (Pa)
R	gas constant ($8.314\,J\,mol^{-1}\,K^{-1}$)
R_1	radius of the evaporating cylinder (m)
T	temperature (K)
T_F	feed temperature (K)
T_s	surface temperature (K)
T_w	wall temperature (K)
v	velocity ($m\,s^{-1}$)
W	residue ($mol\,s^{-1}$)
$\Delta_{evp}H$	heat of evaporation ($J\,mol^{-1}$)
y	coordinate perpendicular to axis of evaporator cylinder (m)
Δy	discrete step in the direction of y coordinate (m)
z	coordinate parallel with evaporator cylinder (m)
Δz	discrete step in the direction of z coordinate (m)

Greek letters

Γ	peripheral liquid load ($l\,dm^{-1}\,h^{-1}$)
λ	thermal conductivity ($W\,m^{-1}\,K^{-1}$)
ν	kinematic viscosity ($m^2\,s^{-1}$)
ρ	density ($kg\,m^{-3}$)
ϑ	conductivity member ($m^2\,s^{-1}$)

References

[1] A. Bose, H.J. Palmer, Ind. Eng. Chem. Fundam. 23 (1984) 459.
[2] Z. Kawala, K. Stephan, Chem. Eng. Technol. 12 (1989) 406.
[3] J.R. Ferron, M. Bhandarkar, Ind. Eng. Chem. Res. 29 (1991) 998.
[4] C.B. Batistella, M.R.W. Maciel, Comp. Chem. Eng. 20 (1996) Suppl. S19–S24.
[5] R. Toei, M. Okazaki, M. Asaeda, J. Chem. Eng. Japan 4 (1971) 188.
[6] M. Micov, J. Lutišan, J. Cvengroš, Sep. Sci. Technol. 32 (1997) 3051.
[7] J. Lutišan, M. Micov, J. Cvengroš, Sep. Sci. Technol. 33 (1998) 83.
[8] J.D. Hoffman, Numerical Methods for Engineers and Scientists, McGraw-Hill, New York, 2nd Edition, 1993, ISBN 0-07-029213.
[9] N.V. Kopchenova, I.A. Maron, Computational Mathematics, 4th Edition, Mir, Moscow, 1987.